

## **NUMERICAL SIMULATION OF NAVIER-STOKES EQUATIONS USING MAC METHOD IN CONFINED INCOMPRESSIBLE FLOWS**

Fernanda Paula Barbosa Pola<sup>1</sup> §, Ives Renê Venturini Pola

University of São Paulo

Instituto de Ciências Matemáticas e de Computação

Avenida Trabalhador São-Carlense

400 - Centro, São Carlos, SP, BRAZIL

**Abstract:** The research area of fluid mechanics is a very interest subject in many engineering applications. First, most problems aimed at studying fluid flows experimentally, and later numerical studies appeared after the mathematical modeling by the Navier-Stokes equations arise. This paper studies the numerical solution of the Navier-Stokes movement and continuity equations for incompressible, confined steady state flows. We used a method based on staggered grids, the MAC (Mark and Cell) method, applied on confined isothermal incompressible flows. But, an alternative approach were employed for the Poisson equation in temporal advance of pressure in the original proposal, basing on a pressure iteration approach. We performed numerical experiments by using two classic problems, the backward-facing step and the lid-driven cavity-flow and presented results for the selected applications.

**AMS Subject Classification:** 35Q30, 76M20

**Key Words:** Navier-Stokes equations, numerical simulation, computational fluid dynamics

### **1. Introduction**

The simulation of the fluid flow problems are mostly based in the usage of the Navier-Stokes equations, which are highly non-linear, coupled to the mass conservation and

---

Received: July 29, 2015

© 2015 Academic Publications

§Correspondence author

energy equations. Together with a proper initial and boundary conditions, the Navier-Stokes equations allow obtaining an interesting result front real applications. Unfortunately, analytical solutions of these equations are only possible in a few simplified cases.

The numeric simulation of a fluid flow can be superficially summarized in a few steps: Given a physical problem, we use a mathematical model through the governing equations and then perform a discretization, obtaining an approximated solution. The main advantages of the numerical simulation are low cost of simulation, temporal evolution analysis and the possibility of simulation using complex geometries. Many effort were dedicated for providing sufficient conditions for the global regularity of the Navier-Stokes equations (for details see, for example, the books [7],[2], and references therein).

The MAC (Marker and Cell) method was proposed by Harlow and Welch [4] for the incompressible simulations with Newtonian fluids in free surface cases, where particles known as markers define the position of the free surface of the fluid. While some works proposed simplified models [5], a survey on the subject can be found on [8]. However, the lack of a free surface does not restrain its usage, being this method one of the most used explicit formulation for the numeric solution of Navier-Stokes equations. The regular MAC method uses a staggered grid and a Poisson equation solution is used to the temporal advance of pressure in the problem domain.

This paper uses an alternative approach for the temporal advance of pressure, instead of using a Poisson equation we use a pressure iteration [1][3]. The paper layout is organized as follows: Section 2 shows the governing equations, the numerical formulation for the MAC method, the pressure iteration approach for time advance, boundary conditions for the simulations in experiments and stability conditions for the execution of the simulation. Section 3 shows the results of the simulations and finally Section 4 draws conclusions on this study.

## 2. Governing Equations

The two-dimensional incompressible fluid flows on Newtonian fluids can be represented by the Navier-Stokes equations

$$\begin{aligned}\frac{\partial u}{\partial t} + \frac{\partial u^2}{\partial x} + \frac{\partial uv}{\partial y} &= -\frac{\partial p}{\partial x} + \nu \left( \frac{\partial^2 u}{\partial x^2} + \frac{\partial^2 u}{\partial y^2} \right) \\ \frac{\partial v}{\partial t} + \frac{\partial vu}{\partial x} + \frac{\partial v^2}{\partial y} &= -\frac{\partial p}{\partial y} + \nu \left( \frac{\partial^2 v}{\partial x^2} + \frac{\partial^2 v}{\partial y^2} \right)\end{aligned}\tag{1}$$

and the continuity equation

$$\frac{\partial u}{\partial x} + \frac{\partial v}{\partial y} = 0, \quad (2)$$

where  $p$  is the pressure to the constant density ( $m^2/s^2$ ),  $u$  and  $v$  are the component of the fluid velocities, respectively to the directions  $x$  and  $y$  in the mapped problem domain. Note that Eqs. (1) and (2) are represented in a cartesian system of coordinates and  $\nu$  is the cinematic viscosity ( $m^2/s$ ) of the Newtonian fluid. Here, we simplify the problem by not considering the gravitational field force.

## 2.1. Numerical Formulation

In MAC method, the computational domain is divided in a finite set of rectangular cells, each one with dimensions  $\delta x$  and  $\delta y$ , forming an uniform grid.

Each cell is indexed by its position  $(i, j)$  in relation with a reference cell, usually adjacent to the origin of the coordinate system. In this work, this cell is chosen so that the origin corresponds to its right upper corner, where the center coordinates of each cell is given by  $(i, j) = ((i - 1/2)\delta x, (j - 1/2)\delta y)$ . The corresponding cells in the interior of the domain are numbered from 1 to  $N_i$  in direction  $x$  and from 1 to  $N_j$  in direction  $y$ , where the cell positions vary depending on the problem, as showed in Figures 1 and 2. The components of the flow velocity are calculated in the horizontal and vertical faces of each cell, and the pressure in its center, characterizing the staggered grid, as can be seen in Figure 3.

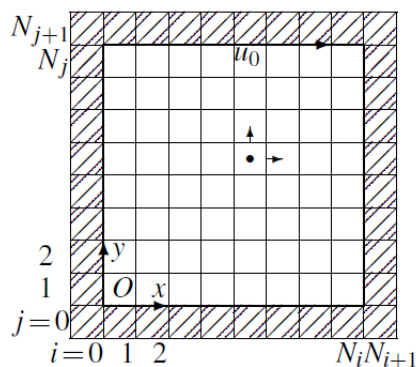


Figure 1: Computational domain of the lid-driven cavity-flow.

The components of the flow velocity are calculated in the horizontal and vertical faces of each cell, and the pressure in its center, characterizing the staggered grid, as can be seen in Figure 3.

The choice for the staggered grid instead of a collocated grid is due to the decoupling of the equations and the resulting generation of oscillatory fields generation for the pressure for the latter.

The solution is evaluated through the advance in time step  $\delta t$  of the variables of the fluid flow, small enough to ensure the stability conditions, as detailed in Section 2.4. This can be achieved in two parts.

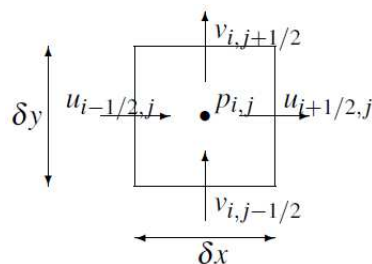


Figure 3: Cell  $(i, j)$  of MAC method

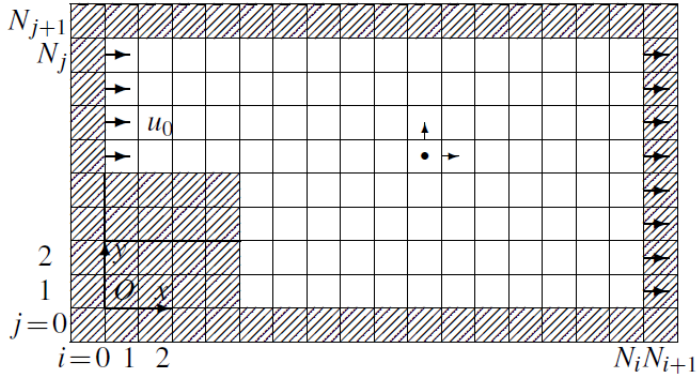


Figure 2: Computational domain of backward-facing step flow.

Initially, the velocity components are updated in all cells  $(i, j)$  of the domain, except for those specified by boundary conditions. In MAC, this evaluation is explicit, being the advance in time based on the solution obtained in the previous time step. The obtained velocities from the first item does not necessary satisfy the continuity Eq. (2). In this part, the velocities components are adjusted to ensure the mass conservation. Such correction is performed by updating the pressure in each cell  $(i, j)$ .

The original MAC method obtains the value of the pressure from the second part by the solution a Poisson equation. We use an alternative which is to perform iterations in the velocities and pressures fields at the same time, until the mass conservation satisfies. This technique is called pressure iteration and is described next.

Initially, the velocity components  $u$  e  $v$  in each cell  $(i, j)$  are estimated by the following finite difference equations:

$$\begin{aligned} u_{i+1/2,j}^{n+1,(0)} &= u_{i+1/2,j}^n + \delta t \left( -\text{CONV}_{i+1/2,j}^n + \frac{1}{Re} \text{VISC}_{i+1/2,j}^n - \frac{p_{i+1,j}^n - p_{i,j}^n}{\delta x} \right) \\ v_{i,j+1/2}^{n+1,(0)} &= v_{i,j+1/2}^n + \delta t \left( -\text{CONV}_{i,j+1/2}^n + \frac{1}{Re} \text{VISC}_{i,j+1/2}^n - \frac{p_{i,j+1}^n - p_{i,j}^n}{\delta y} \right), \end{aligned} \quad (3)$$

where the convective terms are given by

$$\begin{aligned}\text{CONV}_{i+1/2,j}^n &= \frac{(uu)_{i+1,j}^n - (uu)_{i,j}^n}{\delta x} + \frac{(uv)_{i+1/2,j+1/2}^n - (uv)_{i+1/2,j-1/2}^n}{\delta y} \\ \text{CONV}_{i,j+1/2}^n &= \frac{(vu)_{i+1/2,j+1/2}^n - (vu)_{i-1/2,j+1/2}^n}{\delta x} + \frac{(vv)_{i,j+1}^n - (vv)_{i,j}^n}{\delta y}\end{aligned}$$

and the viscous terms by

$$\begin{aligned}\text{VISC}_{i+1/2,j}^n &= \frac{u_{i+3/2,j}^n - 2u_{i+1/2,j}^n + u_{i-1/2,j}^n}{\delta x^2} + \frac{u_{i+1/2,j+1}^n - 2u_{i+1/2,j}^n + u_{i+1/2,j-1}^n}{\delta y^2} \\ \text{VISC}_{i,j+1/2}^n &= \frac{v_{i+1,j+1/2}^n - 2v_{i,j+1/2}^n + v_{i-1,j+1/2}^n}{\delta x^2} + \frac{v_{i,j+3/2}^n - 2v_{i,j+1/2}^n + v_{i,j-1/2}^n}{\delta y^2}.\end{aligned}$$

The convective terms are related with the velocity components where they are not defined in the discretization. The evaluation of such terms is performed by the following

$$\frac{(uu)_{i+1,j}^n - (uu)_{i,j}^n}{\delta x} = \frac{u_{i+1,j}^n \bar{u}_{i+1,j}^n - u_{i,j}^n \bar{u}_{i,j}^n}{\delta x}, \quad (4)$$

considering the first convective term of the momentum equation in the  $x$  direction, and so on. The values of  $\bar{u}_{i+1,j}^n$  and  $\bar{u}_{i,j}^n$  are approximated by the mean of values of  $u$  in the neighborhood points, in which are defined in the discretization, and the values of  $u_{i+1,j}^n$  and  $u_{i,j}^n$  are obtained by using a convective schemes.

This particular approach has a physical reason. Consider the term  $(uu)_{i,j}^n$ . This term represents the transport of the property  $u$  by velocity of convection  $u$  in the center of cell  $(i, j)$ . In other words, according with such product, the property  $u$  is being transported with velocity  $u$ . This becomes clear when we consider the momentum equation in the direction  $x$  under a non-conservative form, given by

$$\frac{\partial u}{\partial t} + \underbrace{u \frac{\partial u}{\partial x} + v \frac{\partial u}{\partial y}}_{\text{CONV}} = -\frac{\partial p}{\partial x} + \frac{1}{Re} \left( \frac{\partial^2 u}{\partial x^2} + \frac{\partial^2 u}{\partial y^2} \right).$$

According with the above expression, it can be seen the transport of the property  $u$  by the convective terms along the directions  $x$  and  $y$  with velocity components  $u$  and  $v$ , respectively.

The separation of  $(uu)_{i,j}^n$  in form  $u_{i,j}^n \bar{u}_{i,j}^n$  is also a way to make the finite difference equations linear, because the product  $u_{i,j}^n \bar{u}_{i,j}^n$  is linear with relation with  $u_{i,j}^n$ . Hirt and Cook considered that  $u_{i,j}^n = \bar{u}_{i,j}^n$ , making use of the mean of velocities in neighbor points, but clarifying that the resulting equations will only be stable as long as the a

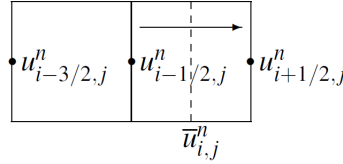
sufficient viscosity be applied, i.e., the numerical results will be acceptable only for low numbers of Reynolds. Based in those arguments, we use the CUBISTA scheme [6] for the approximation of convective terms. Then, considering the term  $(uu)_{i,j}^n$ , we proceed as the follows.

Consider the term  $\bar{u}_{i,j}^n$ , given by

$$\bar{u}_{i,j}^n = \frac{u_{i+1/2,j}^n + u_{i-1/2,j}^n}{2}. \quad (5)$$

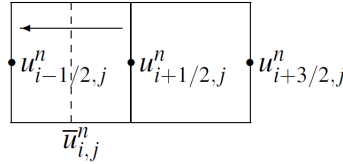
- If  $\bar{u}_{i,j}^n > 0$ , it is defined

$$u_D = u_{i+1/2,j}^n \quad u_U = u_{i-1/2,j}^n \quad u_R = u_{i-3/2,j}^n$$



- If  $\bar{u}_{i,j}^n < 0$ , it is defined

$$u_D = u_{i-1/2,j}^n \quad u_U = u_{i+1/2,j}^n \quad u_R = u_{i+3/2,j}^n$$



Note that  $D$  indicate the downstream,  $U$  the upstream and  $R$  the remote upstream.

Let  $\hat{u} = \frac{u_U - u_R}{u_D - u_R}$ . Then,

$$u_{i,j}^n = \begin{cases} \frac{1}{4}(7u_U - 3u_R), & \text{se } 0 < \hat{u} < \frac{3}{8} \\ \frac{1}{8}(3u_D + 6u_U - u_R), & \text{se } \frac{3}{8} \leq \hat{u} \leq \frac{3}{4} \\ \frac{1}{4}(3u_D + u_U), & \text{se } \frac{3}{4} < \hat{u} < 1 \\ u_U, & \text{otherwise} \end{cases}$$

The evaluation of  $u_{i+1,j}^n$  is done in a similar way, including the other components of the convective terms.

## 2.2. Pressure Iteration

Once estimated the velocity components  $u_{i+1/2,j}^{n+1,(0)}$  and  $v_{i,j+1/2}^{n+1,(0)}$  for all the cells, we have to adjust such components by the pressure iteration, as follows.

Given an iteration  $k$  of the simulation, the dilation  $D_{i,j}^{n+1,(k)}$  in each cell  $(i,j)$  is calculated as

$$D_{i,j}^{n+1,(k)} = \frac{u_{i+1/2,j}^{n+1,(k)} - u_{i-1/2,j}^{n+1,(k)}}{\delta x} + \frac{v_{i,j+1/2}^{n+1,(k)} - v_{i,j-1/2}^{n+1,(k)}}{\delta y}.$$

The dilation is proportional to the mass flux in each cell, so if the dilation is null in all cells, the Continuity Equation (Eq. (2)), in which the second term of the above equation represents its discretization under finite differences, is satisfied in all the domain and the flow is incompressible. In order to verify that, consider the maximum dilation obtained in the domain, and if

$$\max_{i,j} |D_{i,j}^{n+1,(k)}| \geq \varepsilon,$$

where  $\varepsilon$  is a defined precision, the flow must not be considered incompressible and adjusts are necessary. Usually,  $\varepsilon = \sigma_1/N$ , where  $N$  is the number of cells in the computational domain. In this paper, it is considered  $\sigma_1 = 10^{-7}$ .

The aforementioned adjusts are made in the following way. First, the pressure is updated in each cell by

$$p_{i,j}^{n+1,(k+1)} = p_{i,j}^{n+1,(k)} + \delta p_{i,j}^{(k)},$$

where

$$\delta p_{i,j}^{(k)} = \frac{-\beta_0 D_{i,j}^{n+1,(k)}}{2\delta t \left( \frac{1}{\delta x^2} + \frac{1}{\delta y^2} \right)}$$

and  $p_{i,j}^{n+1,(0)} = p_{i,j}^n$ .  $\beta_0$  is a relaxation factor, with limits  $0 < \beta_0 < 2$ . We used  $\beta_0 = 1$ .

The velocity components, except for those defined in the boundary, are updated by

$$\begin{aligned} u_{i+1/2,j}^{n+1,(k+1/2)} &= u_{i+1/2,j}^{n+1,(k)} + \frac{\delta t}{\delta x} \delta p_{i,j}^{(k)} \\ u_{i-1/2,j}^{n+1,(k+1)} &= u_{i-1/2,j}^{n+1,(k+1/2)} - \frac{\delta t}{\delta x} \delta p_{i,j}^{(k)} \\ v_{i,j+1/2}^{n+1,(k+1/2)} &= v_{i,j+1/2}^{n+1,(k)} + \frac{\delta t}{\delta y} \delta p_{i,j}^{(k)} \\ v_{i,j-1/2}^{n+1,(k+1)} &= v_{i,j-1/2}^{n+1,(k+1/2)} - \frac{\delta t}{\delta y} \delta p_{i,j}^{(k)}. \end{aligned}$$

During the traversing process on the cells, the velocity components are updated twice. Therefore, the first update refer to a component to the level  $(k + 1/2)$  in above equations, being the definitive to the  $(k + 1)$ .

After the pressure and velocity update, we increment  $k$  repeating the process until

$$\max_{i,j} \left| D_{i,j}^{n+1,(k)} \right| < \varepsilon.$$

Once this condition is satisfied at  $(k) \equiv (K)$ , then

$$u_{i+1/2,j}^{n+1} = u_{i+1/2,j}^{n+1,(K)} \quad v_{i,j+1/2}^{n+1} = u_{i,j+1/2}^{n+1,(K)} \quad p_{i,j}^{n+1} = p_{i,j}^{n+1,(K)}.$$

Therefore, when the pressure iteration is concluded, all variables were advanced in time, so  $n$  is incremented to the next temporal step. The process must be repeated until the stationary state is achieved. Such condition can be verified by calculating the residue  $\text{RES}^{n+1}$

$$\text{RES}^{n+1} = \sum_i \sum_j \left( \left| u_{i+1/2,j}^{n+1} - u_{i+1/2,j}^n \right| + \left| v_{i,j+1/2}^{n+1} - v_{i,j+1/2}^n \right| \right) \leq \xi,$$

where  $\xi$  is the defined precision. Usually,  $\xi = \sigma_2/N$  where  $N$  is the number of cells in the computational domain. In this paper, we adopted  $\sigma_2 = 10^{-5}$ .

### 2.3. Boundary Conditions

The boundary conditions used in this paper apply to both studied cases. We used non-slip conditions for rigid walls, then the tangential velocity in wall  $v_t = 0$ . But, for the MAC method, the tangential velocity to the wall is not defined in adjacent points to the wall, so we consider  $v_t|_{\text{Ext}} = -v_t|_{\text{Int}}$ , where Int and Ext are the points in the adjacent cells to the boundary, internal and external the domain, respectively, as seen in Figure 4. Then, during the calculation of the convective terms

$$\bar{v}_t|_{\text{wall}} = \frac{v_t|_{\text{Int}} + v_t|_{\text{Ext}}}{2} = 0. \quad (6)$$

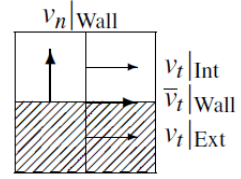


Figure 4: Rigid wall velocities.

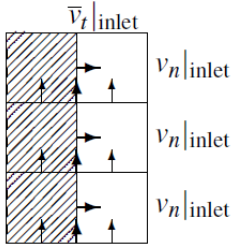


Figure 5: Inlet normal and tangential velocity.

The wall is considered impermeable, and the adjacent normal velocity is null  $v_n|_{\text{wall}} = 0$ . For moving walls at velocity  $v_0$  or rigid slip walls where the fluid in contact moves with the same velocity, we have  $v_t = v_0$ , then we have the condition  $v_t|_{\text{Ext}} = 2v_0 - v_t|_{\text{Int}}$ . Therefore,  $\bar{v}_t|_{\text{wall}} = \frac{v_t|_{\text{Int}} + v_t|_{\text{Ext}}}{2} = v_0$ . The normal velocity is null as in the previous case.

In the inlet of the domain, the normal and tangential velocity are  $v_n|_{\text{inlet}} = f_t$  and  $\bar{v}_t|_{\text{inlet}} = g_t$ , where  $f_t$  and  $g_t$  are known, usually from the tangential direction of the to the inlet, but they can also be set constant, as in the inlet of the backward-facing step problem.

Usually, it is considered that the fluid enters in the normal direction to the wall, so  $g_t \equiv 0$  and we assume the Eq. (6) to the tangential velocity. They can be seen in Figure 5.

For the outlet part of the boundary conditions, there are many ways to set up it. But, commonly it is assumed that there is no variation of the velocity components in the normal direction to the exit, i.e.

$$\left. \frac{\partial v_t}{\partial \hat{n}} \right|_{\text{outlet}} = 0 \quad \left. \frac{\partial v_n}{\partial \hat{n}} \right|_{\text{outlet}} = 0.$$

Therefore, we apply the conditions

$$v_t|_{\text{Int}} = v_t|_{\text{Ext}} \quad v_n|_{\text{outlet}} = v_n|_{\text{Int}},$$

where the velocity is represented as in the Figure 6.

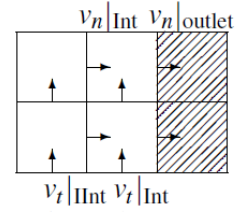


Figure 6: Outlet normal and tangential velocity.

## 2.4. Stability Conditions

The explicit formulation of the MAC method produces some restrictions about the value of  $\delta t$ . They are described as follows.

The flow must not cross more than one cell in any direction at each time step, resulting in

$$\delta t_1 < \min \left( \frac{\delta x}{|u|_{\max}}, \frac{\delta y}{|v|_{\max}} \right). \quad (7)$$

This restriction is due to the fact that the convective approximations assume variations only between adjacent cells.

The diffusive term in the momentum equations demands that

$$\delta t_2 < \frac{Re}{2} \left( \frac{1}{\delta x^2} + \frac{1}{\delta y^2} \right)^{-1}. \quad (8)$$

Hirt and Cook showed by means of linear analysis that

$$\delta t_3 < \frac{2}{Re \max(|u|_{\max}^2, |v|_{\max}^2)}. \quad (9)$$

Finally,  $\delta t$  satisfies the restrictions (7), (8) and (9) if

$$\delta t \leq \min(\delta t_1, \delta t_2, \delta t_3).$$

In this paper, we update  $\delta t$  at each time step by

$$\delta t = \tau \min(\delta t_1, \delta t_2, \delta t_3), \quad (10)$$

with  $0 < \tau < 1$ , and  $\delta t_1, \delta t_2, \delta t_3$  given though the Eqs.(7)-(9) converted in equals. All simulations were executed with  $\tau = 0.5$ .

### 3. Numeric Results

In this section a numeric solution of Navier-Stokes and continuity equations is evaluated, in confined isotherm and incompressible flows, using the modified MAC method presented in above sections. We investigate two classic problems, the lid-driven cavity-flow and the backward-facing step, both in transient state.

In the lid-driven cavity-flow, a fluid that is initially in steady state with cinematic viscosity  $\nu$  is retained in a squared cavity of size  $L$ , filling it at maximum. Suddenly, the lid begins to move with velocity  $U_0$ , according with Figure 7. The walls are all rigid and impermeable, but the lateral and inside ones are non-slip, and the top moving lid non-slip, being only treated as slip where the fluid flows with velocity  $U_0$ . The used Reynolds value for this simulation is given by  $Re = \frac{U_0 L}{\nu}$ .

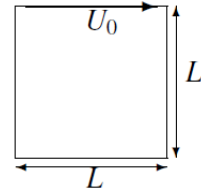


Figure 7: Lid-driven cavity-flow problem.

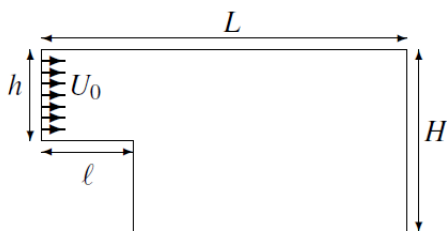


Figure 8: Backward-facing step problem.

affected by the step, so when it leaves the region above the step, the fluid occupies all area of the section  $H$ , creating a recirculation zone in lateral wall proximity.

We assumed that  $\alpha = \ell/L$  is given by  $\alpha = 1/4$ , and that  $h/H = 1/2$ , making the step half of the region height, and a quarter of width. The Reynolds number for this case is given by  $Re = \frac{U_0 h}{\nu}$ .

For the experiments, we used simulations using Reynolds values 1, 10 and 100. The stationary state is obtained after 17501, 18219 e 4493 iterations, respectively, where the residue falls proportionally the number of iterations for the tested Reynolds values. These results are shown in Figure 9.

For the Backward-facing step problem, the simulations were executed using the same values of Reynolds. In this case, the behavior of residue is more dependant on the Reynolds value, and values above 100 caused numerical instability. Instead of refining the mesh in order to attenuate the instability, forcing the number of iterations used without need, we reduced the  $\tau$  factor in the Eq. (10) for smaller values. Then, the stationary state is achieved after 5400, 5898 e 3447 time steps, respectively for Reynolds  $Re = 1, 10$  e 100. The results for this measure can be seen in the Figure 10.

In the backward-facing step problem, a fluid with cinematic viscosity  $\nu$  fills a region of width  $L$  with a step of width  $\ell$ , as showed in the Figure 8. Then, the fluid flows into inlet with a velocity  $U_0$  in a region of transversal section  $h$ . The incompressibility forces the same quantity of fluid that entries through this region flows outside through a transversal section  $H$ . The fluid flow inside this region is affected

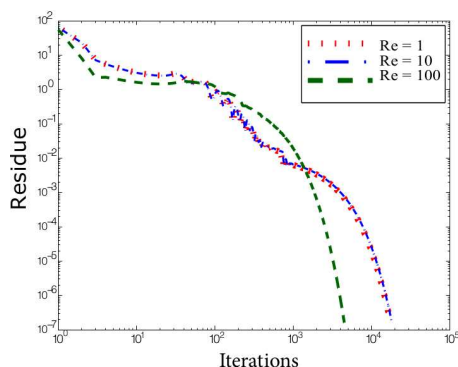


Figure 9: Residue measure from Lid-driven cavity-flow problem.

Finally, additional results obtained by the simulations are presented. We measured the flow vector field, velocity components  $u$  and  $v$  and the pressure rate  $p$  for both cases simulated. The values of pressure are in relation with the initial pressure. For the Lid-driven cavity-flow problem, these results are presented in Figures 11 to 14, while the Figures 15 to 18 present these results for the Backward-facing step problem.

Results from the Lid-driven cavity-flow problem show that the flow inside the cavity has viscosity and inertial forces that induce its recirculation due to the moving slip. For both simulated Reynolds values, it can be seen the occurrence of secondary but smaller recirculation fields in the lower corners.

Regarding the Backward-facing step problem results with  $Re = 10$ , the viscous terms of Navier-Stokes equations have more influence than the convective ones. The boundary layer of velocity component  $x$  has low gradient and then it become thick. But, in the case of simulation with  $Re = 100$ , it can be noted a fluid flow less characterized by the viscosity, where the recirculation can be seen from the negative values for the velocity component  $y$  and the flow vector field plots.

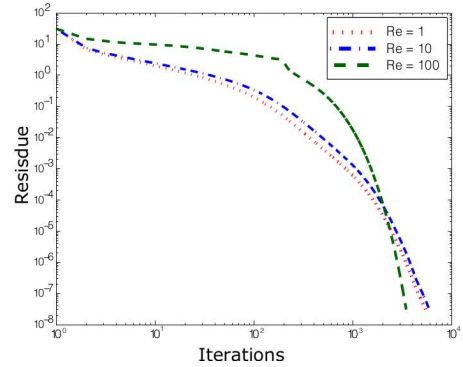


Figure 10: Residue measure from Backward-facing step problem.

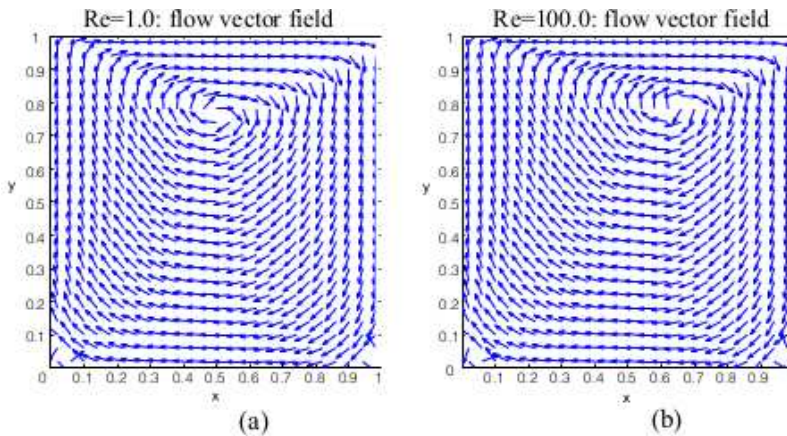


Figure 11: Flow vector fields for the lid-driven cavity-flow problem.

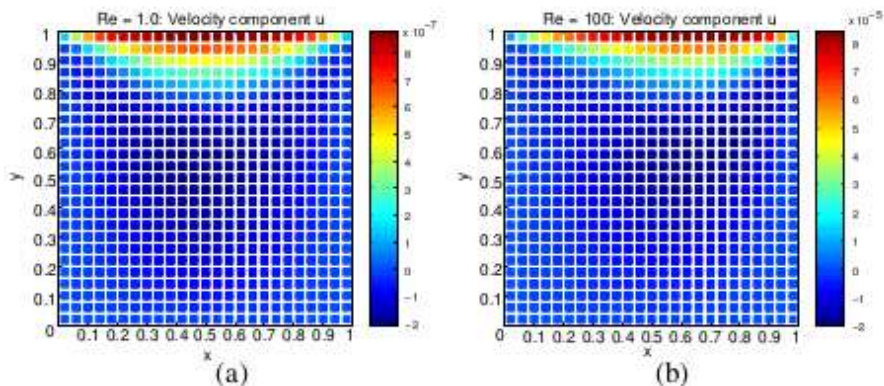


Figure 12: Velocity component  $u$  for the lid-driven cavity-flow problem.

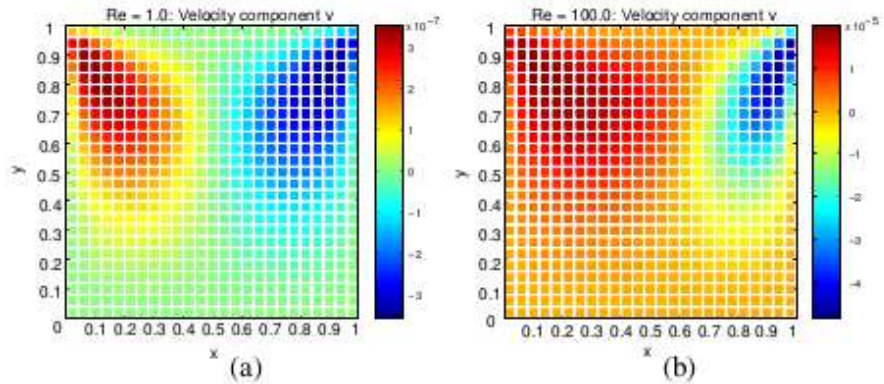


Figure 13: Velocity component  $v$  for the lid-driven cavity-flow problem.

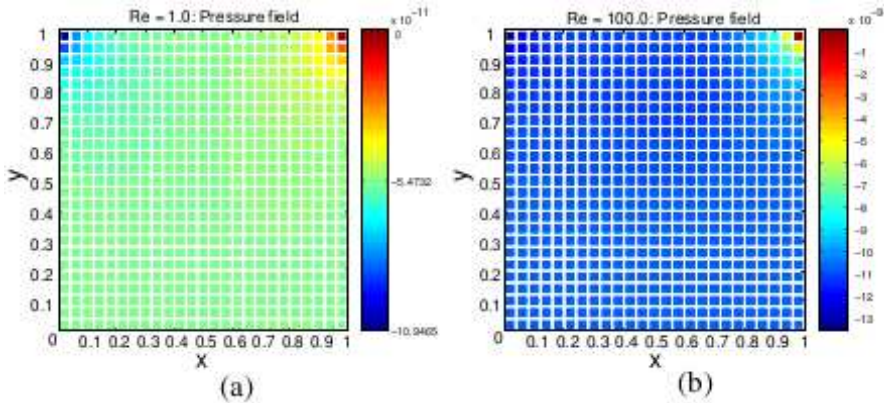


Figure 14: Pressure rate  $p$  at constant density in the lid-driven cavity-flow problem.

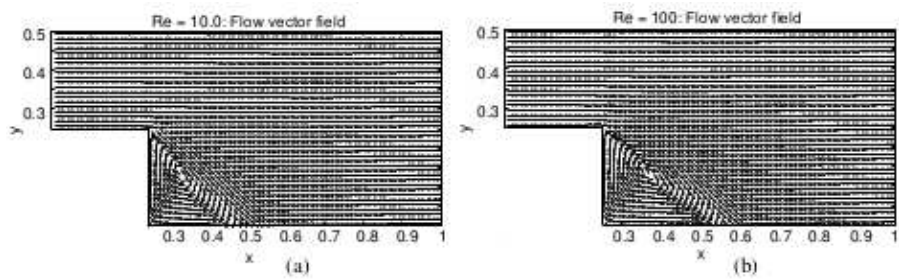


Figure 15: Flow vector fields for the Backward-facing step problem.

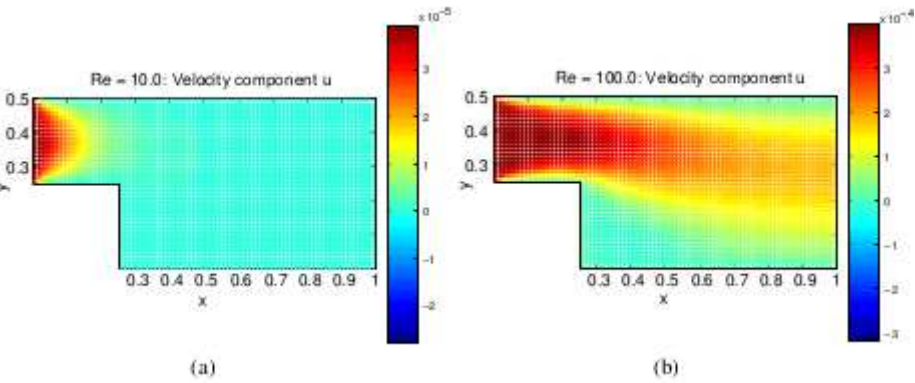


Figure 16: Velocity component  $u$  for the Backward-facing step problem.

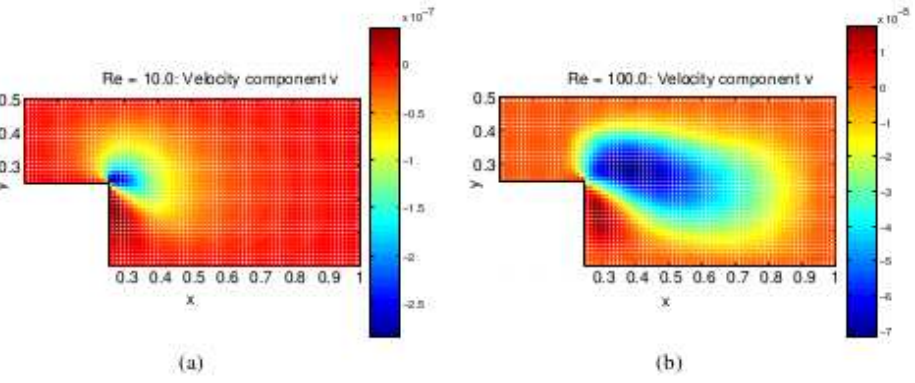


Figure 17: Velocity component  $v$  for the Backward-facing step problem.

#### 4. Conclusion

The solution of the fluid flow problems are based in the usage of the Navier-Stokes equations, which are highly non-linear, coupled to the mass conservation and energy

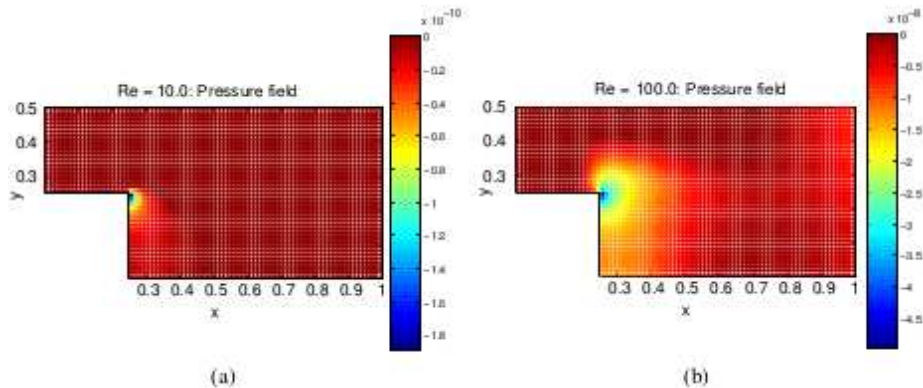


Figure 18: Pressure rate  $p$  at constant density in the Backward-facing step problem.

equations.

The main advantages of the numerical solutions are low cost of simulation, temporal evolution analysis and the possibility of simulation using complex geometries.

In this paper we studied the MAC method using an alternative approach for the temporal advance of pressure, based in the pressure iteration. We presented the governing equations, the numeric formulation for the method and the used pressure iteration procedure.

All boundary conditions were presented, focusing on the cases object of simulation in the experiments. Numerical results were presented to verify the stability of the method for different Reynolds values in the test cases.

## References

- [1] A. J. Chorin, *AEC Research and Development Report*, NYO-1480-61 (1966).
- [2] C. Foias, O. Manley, R. Rosa, and R. Temam, *Navier-Stokes Equations and Turbulence*, Encyclopedia of Mathematics and its Applications. Cambridge University Press (2001).
- [3] C. W. Hirt, Heuristic stability theory for finite-difference equations, *Journal of Computational Physics*, **2** (1968), 339–355.
- [4] F. H. Harlow and J. E. Welch, Numerical calculation of time-dependent viscous incompressible flow of fluid with free surface. *Physics of Fluids*, **8** (1965), 2182–2189.

- [5] L. Cheng and S. Armfield, A simplified marker and cell method for unsteady flows on non-staggered grids, *International Journal for Numerical Methods in Fluids*, **21**, No 1 (1995), 15–34.
- [6] M. A. Alves, P. J. Oliveira, and F. T. Pinho, A convergent and universally bounded interpolation scheme for the treatment of advection, *International Journal for Numerical Methods in Fluids*, **41** (2003), 47–75.
- [7] R. Temam, *Navier-Stokes Equations: Theory and Numerical Analysis*. AMS / Chelsea Publication (2001).
- [8] S. McKee, M. Tomé, V. Ferreira, J. Cuminato, A. Castelo, F. Sousa, and N. Mangiavacchi, The MAC method, *Computers & Fluids*, **37**, No 8 (2008), 907–930.